

RESEARCH

Open Access

Forecasting the next handoff for users moving with the Random Waypoint mobility model

Enrica Zola*, Francisco Barcelo-Arroyo and Israel Martín-Escalona

Abstract

Users in a cellular network can move while their connections are handed off to different access points. Studies prove that the mobility pattern followed have a strong impact on performance metrics (i.e., handoff (HO) rate, cell residence time). Recently, some key aspects of the Random Waypoint mobility model have been studied in depth, but relating those studies with different cellular layouts has not been reported. Interest in forecasting the cell to which a device may be handed off depending on the movement pattern is twofold. First, it gives insight into properties and statistics of the mobility model. Second, and from a more practical perspective, it is useful to manage resource allocation and reservation strategies in order to smooth the HO process. The goal of this article is to provide an analytical framework for these predictions in a simple layout. Given a node's current location and the timestamp and location of the last waypoint, an approximation for HO during time Δt is derived. The analysis is provided along with numerical examples and simulations for a symmetrical layout and uniform speed distribution. Results shed light on how useful more advanced strategies can be.

Keywords: Handoff probability forecast, Random Waypoint mobility model, Analytical framework

1. Introduction

Users in a cellular network move while their connections are transferred between access points. This process is known as handoff (HO). This same concept holds for different technologies (e.g., GSM, UMTS, LTE, WiFi, ZigBee, WiMAX), although the name of the key element changes according to the specific standard (e.g., base station—BS, node B, access point—AP). As the user moves, the quality of the signal received from the current cell may decrease under some acceptable threshold. This event will trigger the HO procedure [1]. The time needed to transfer the ongoing communications to the new cell is crucial [2,3] since if this process lasts too long the user may suffer degradation in the quality of the ongoing services. In some cases, it may lead to a drop in the communication [4]. This issue is particularly important for delay-sensitive applications such as video and audio streaming.

Mobility prediction techniques allow the network to prepare for the HO in advance (e.g., booking resources for the expected HO in the destination cell) [5]. Resource demands could fluctuate abruptly due to the

movement of high data rate users. If one can predict requests of bandwidth at a cell, the overall network performance would improve. The goal of our research is to provide a mathematical framework through which the percentage of HO for users moving with a known mobility pattern can be forecasted. By properly handling this information at the BSs, the network can better manage the resources and prepare the HOs, hence reducing the time needed to authenticate in the connection in the new cell and decreasing the probability of dropping the connection. However, how this prediction is used by the network is out of the scope of this article.

Structural approaches study mobility through mathematical models that try to represent human or vehicle mobility. Mobility models play a key role when planning a wireless network (i.e., resource allocation, location updating, and channel holding time). The Random Waypoint (RWP) mobility model [6] is simple and has extensively been used in simulation studies. Kurkowski et al. [7] analyze MANET simulation studies published in a premiere conference for the MANET community between 2000 and 2005. They found that 66% of the studies involving mobility used the RWP mobility model. Despite it has been criticized for not being representative of how humans

* Correspondence: enrica@entel.upc.edu
Telematics Engineering Department, Universitat Politècnica de Catalunya (UPC), Barcelona, Spain

actually move, it is still largely used in many studies [8-13]. Rojas et al. [14] validate the RWP against real mobility data. With small changes to the distributions used in the RWP (e.g., non-uniform distribution of the waypoints), the authors show that it can be used as a good model for mobility in large geographic areas such as a city. Considering that extracting a mobility pattern from real traces is complex and, anyway, it would be specific to the environment and conditions from which it has been extracted, the use of the RWP in simulation studies is widely accepted. Many researchers have studied the impact of the RWP on routing protocols [15,16], connectivity probabilities [17,18], cell residence time [19-21], and cell change rate [20,22]. However, prediction of the probability of HO to a given cell for users moving according to the RWP mobility pattern has not yet been addressed.

In this article, a detailed description of the analytical framework to forecast the next cell to which a user HOs within a certain period of time is provided. The framework was partially presented in [23]. This analysis follows previous research on statistical characteristics of the RWP mobility model (i.e., length and duration of the straight movement between two waypoints [22], node distribution [24,25]). Moreover, simulation results are shown in this study in order to validate the analytical model and check the small impact of the necessary simplifications done. The importance of this study is twofold. First, it provides a deeper insight into the statistics of the RWP mobility model, extending previous analysis [22,24-26]. This statistical knowledge provides a better understanding of the interplay of the mobility pattern with network parameters. Second, and from a more practical perspective, the HO prediction is useful to manage resource allocation and reservation strategies. According to our model, few requirements are needed to perform the forecast of a possible HO in the near future: knowledge of the cells' locations and geometries; knowledge of user's position (e.g., through GPS); knowledge of when and where the user changed direction of movement and speed for the last time (e.g., through inertial sensors). Despite the model has been applied to a 4-cell scenario (see Section 4.3), this methodology can be generalized to any symmetrical layout in which fixed BSs are located at the vertices of any regular polygon. Researchers can take advantage of the prediction framework presented in this article for their simulations. As an example, it can be applied in studies on allocation strategies for QoS improvement in cellular networks.

The remainder of this article is organized as follows. Section 2 provides a brief overview of the related literature. The RWP mobility model is explained in Section 3. The method proposed to estimate the probability of HO to a given cell is shown in Section 4. The method is then applied to different cases: numerical results are provided

in Section 5, while simulation results in Section 6. Section 7 summarizes the main conclusion.

2. Related work

A lot of research has been conducted to propose schemes that try to decrease the HO latencies. This problem is particularly important in IEEE 802.11 networks where it has been proven that these latencies are especially high [2]. Since the scanning time needed to find a new candidate AP is the most constraining phase, many proposals can be found which aim to reduce it. Velayos and Karlsson [3] suggest reducing the link-layer detection time to three consecutive lost frames and to use different timers for the active scanning, thus reducing the search time at least by 20%. An HO procedure is presented in [27], which reduces the discovery phase using a selective scanning algorithm and a caching mechanism. Modification in the standard active scan is proposed in [28]; a user should be able to periodically probe in the background for APs on other channels even when it is already associated with an AP. These make-before-brake algorithms lead to a significant reduction in MAC layer HO overhead. Similarly, in order to limit the frequency of channel scanning, an adaptive mechanism is recommended in [29] to dynamically adjust the threshold triggering the channel scanning operations. In addition to *horizontal HO*, i.e., HO between cells within the domain of a single wireless access technology, recent interest has been directed toward *vertical HO* (VHO), which allows users to HO among heterogeneous wireless access networks [30,31]. Lee et al. [32] investigate the problem of VHO from a 3 G cellular network to a WLAN hotspot. They propose a call admission control that allows the WLAN to limit the VHOs and reduce unnecessary VHO processing. Ben Ali and Pierre [33] evaluate the impact of VHO on the performance of the voice admission control in different mobility environments.

Some research has been targeted to develop models that predict mobile user trajectory, which can be used to allocate resources at the new cell and to aid the HO process. Pathirana et al. [34] propose the use of an extended Kalman filter in the prediction of a mobile user's arrival to the next cell. The technique proposed in [5] uses real-time mobile positioning information and previous HO locations reported by other nodes in order to predict the HO event. With mobility prediction, the reservation at each BS can dynamically be adjusted. They demonstrated that reservation efficiency improves as the knowledge incorporated into the scheme increases. Joshi et al. [35] aim to exploit the notion of predictability and propose algorithms to achieve low latencies while minimizing the message overhead. The prediction technique proposed in [13] uses both simple moving average for (sub-)inertial movements and simple mobility pattern matching for non-inertial movements. An HO prediction

algorithm is designed for eNodeB's HO preparation, thus improving the HO in 3 G LTE systems.

Prediction of users' movement is also possible using trace data [36]. For HO success, the most important predictions occur when moving into highly populated cells. Other studies exploit real traces to analyze the predictability of users' movements inside the network [37,38]. Sricharan and Vaidehi [37] examine real-time mobility traces and identify key mobility parameters. A generic framework for mobility prediction is proposed in [38] where a model is proposed to predict the sequences of a user's path from observed sequences. Libo et al. [39] conducted an extensive empirical comparison of four important classes of location predictors in order to prove which could most accurately predict the next cell for a mobile wireless-network user. They found that the complex predictors were at best only negligibly better than the simple Markov predictor.

Much effort has been made to gain understanding of the implications that the use of the RWP model may cause. The "steady-state" problem has been addressed in [22,40]. By giving a formal description of the RWP model in terms of a discrete-time stochastic process, Bettstetter et al. [22] investigate the length and time of the movement between waypoints, the spatial distribution of nodes, the direction angle at a new waypoint, and the cell change rate. Navidi and Camp [40] derive the stationary distributions for location, speed, and pause time. The spatial node distribution of nodes is also addressed in [24,25]. Given that the RWP tends to bring the nodes to the centre of the area, Bettstetter et al. [24] proposed to initially distribute the nodes according to a given pattern so that the network starts in the steady state. Hyttia et al. [25] propose a general expression for the node distribution without using approximations. An exact formula for the mean arrival rate across an arbitrary curve is presented in [20]. This result, together with the distribution of a node's location, allows the computation of other metrics, such as the mean HO rate and the mean dwell time. Pla and Casares-Giner [19] propose a model of the sojourn time in the overlap area for users moving according to the RWP. To simplify their study, they assume that waypoints cannot fall inside the overlap area. The obtained results show that the common assumption of exponential distribution for this time is not suitable.

3. Random waypoint mobility model

Modeling the mobility of terminals in wireless networks, where the connection has to be handled through several APs, is a key in order to forecast the quality of service and design the necessary resources. In general, high mobility leads to poorer quality of service since more HO that cause extra overhead are performed. While it is obvious

that faster speeds tend to cause more HO, it must be highlighted that the mobility pattern is also related to the HO rate: a terminal moving in circles close to the AP at high speed may not require HO while another one moving away from the AP will certainly require an HO soon.

The RWP was introduced in [6]. In this model, each node is assigned an initial location (WP_0) and a destination (WP_1), which are chosen independently and uniformly within the *whole area* (i.e., the area where nodes can move, which is generally assumed to be convex). A speed (v) is assigned as well, which is chosen uniformly or according to any other distribution from an interval (v_{\min} to v_{\max}) and independent of the initial location and destination. Between the two waypoints WP_0 and WP_1 , the node follows a straight line and moves at a constant speed. The movement between two waypoints is referred to as a *leg* or *transition*. After reaching WP_1 , a new destination and a new speed are chosen independent of previous destinations and speeds. The node may remain paused for some random *pause time* before starting its movement toward the next waypoint. For simplicity, pause times are not considered in this study.

Exact formulas for the probability density function (pdf) of the distance between two waypoints, i.e., pdf of the transition length, $f_L(\ell)$ in different scenarios are provided in [22,25]. According to the geometry and dimensions of the area, the mean distance can be evaluated.

4. Probability of handoff to a given cell

4.1. Problem statement

The objective of the study is to estimate the probability of HO to a given cell before a given period of time (Δt) elapses, provided that we know where and when the last waypoint was reached. The forecast is performed under the following assumptions:

- The whole area A is a circle of radius R , and APs are placed at the corners of a regular polygon inside the circle. Any regular polygon can be considered (e.g., a square as shown in Section 4.3).
- Ideal conditions are considered (i.e., noise and fading are not taken into account).
- Coverage areas have a circular shape.
- Current position P_t at time t is known.
- Position and time of the last waypoint (WP_j at time j) are known (i.e., where and when the node changed to the present direction and speed). Alternatively, movement direction and time of the last waypoint can be used to derive the position of the last waypoint.
- It is assumed that the number of waypoints $X(\Delta t)$ that a node may reach during Δt is smaller or equal to one.
- In general, the node may perform multiple HOs in Δt ; in this study, only the first HO (if any) is studied.

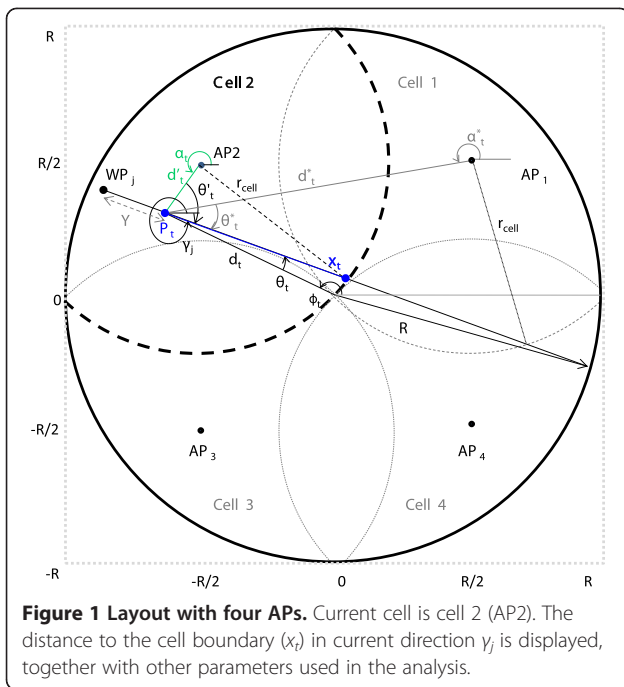


Figure 1 Layout with four APs. Current cell is cell 2 (AP2). The distance to the cell boundary (x_t) in current direction γ_j is displayed, together with other parameters used in the analysis.

- When the node is inside the coverage areas of two or more APs (i.e., overlapping area), the HO starts when the node exits the coverage area of the AP to which it is currently associated. Other HO strategies may be applied, with minor changes in the proposed framework.

The following parameters are considered (a layout with four APs is depicted in Figure 1 for better understanding):

- γ_j represents the current angle of direction and v_j the current speed.
- Y is the distance between WP_j and P_t (i.e., distance already traveled at speed v_j in direction γ_j).
- x_t , x_A , and x_{LAP} represent the distances from P_t to the cell boundaries, the boundaries of A and the borders of the neighboring cell in direction γ_j , respectively (see Figures 1 and 2). The *neighboring cell* is the cell toward which the MN is moving in direction γ_j .
- If there are two intersections with the neighboring cell, they are identified with x_{LAP+} and x_{LAP-} (see Figure 2b).

The definition of a node's movement direction γ_j in a two-dimensional space can be better understood through Figure 1. As shown in [22], the outcome of this angle depends on both polar coordinates of P_t (e.g., d_t and Φ_t). Thus, a second alternative direction angle θ_t is introduced. This angle is defined in a way that $\theta_t = 0$ for movements going through the center of the circular area. A major advantage of this definition is that the outcome of θ_t is independent of the polar angle Φ_t . It can directly be mapped onto γ_j for a given Φ_t . If we define that counterclockwise angles count positive

$$\gamma_j = \theta_t + \phi_t + \pi. \quad (1)$$

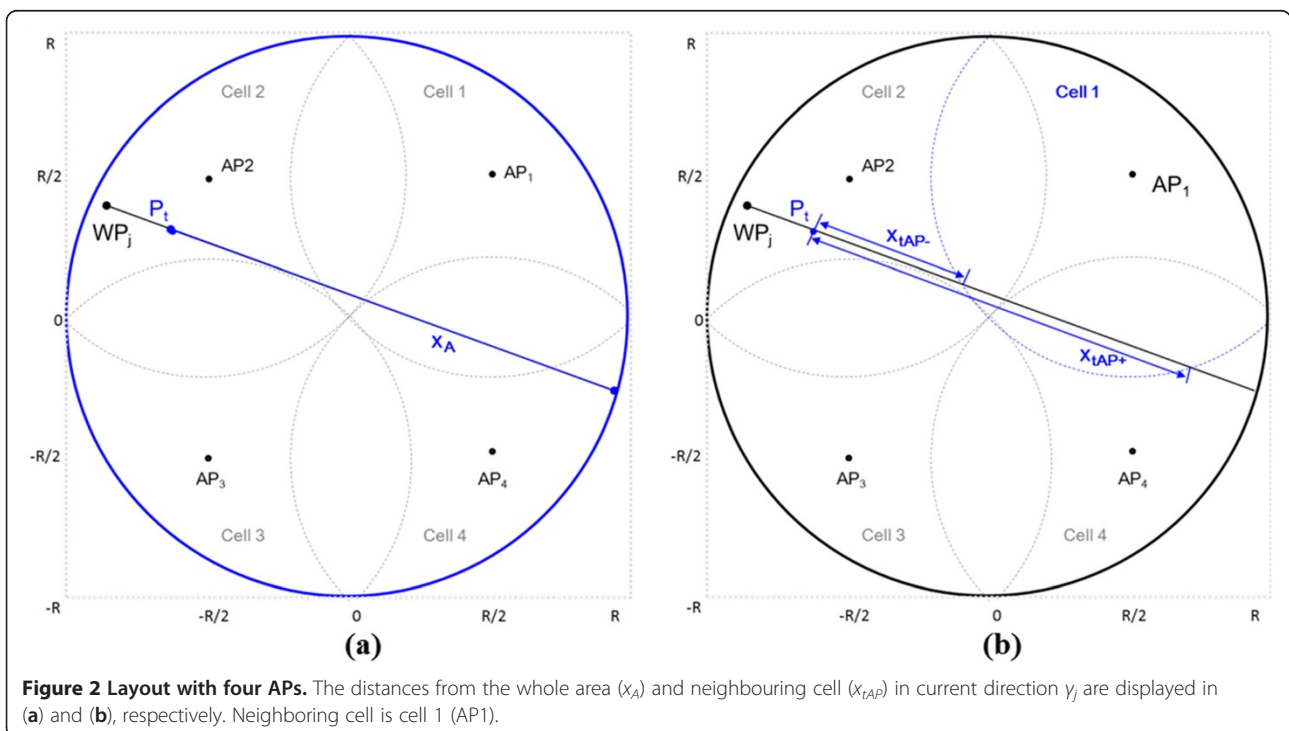


Figure 2 Layout with four APs. The distances from the whole area (x_A) and neighbouring cell (x_{LAP}) in current direction γ_j are displayed in (a) and (b), respectively. Neighboring cell is cell 1 (AP1).

In a circular layout, the formula for the maximum length of the movement from P_t in direction γ_j (i.e., x_A according to previous definition) is [22]

$$x_A(\theta_t) = d_t \cdot \cos\theta_t + \sqrt{R^2 - (d_t \cdot \sin\theta_t)^2}, \quad (2)$$

where d_t and Φ_t are the polar coordinates of current position P_t with respect to the center of A . Similarly

$$x_t(\theta'_t) = d'_t \cdot \cos\theta'_t + \sqrt{r_{\text{cell}}^2 - (d'_t \cdot \sin\theta'_t)^2}, \quad (3)$$

$$\begin{cases} x_{tAP+}(\theta_t^*) = d_t^* \cdot \cos\theta_t^* + \sqrt{r_{\text{cell}}^2 - (d_t^* \cdot \sin\theta_t^*)^2} \\ x_{tAP-}(\theta_t^*) = d_t^* \cdot \cos\theta_t^* - \sqrt{r_{\text{cell}}^2 - (d_t^* \cdot \sin\theta_t^*)^2} \end{cases}, \quad (4)$$

where d'_t is the distance of P_t to the center of the current cell, $\theta'_t = \gamma_j - \alpha_t - \pi$ (see Figure 1), α_t is the angle of P_t with respect to the center of the cell, r_{cell} is the radius of the cell, d_t^* is the distance of P_t to the center of the neighboring cell (i.e., cell 1 in Figure 2), $\theta_t^* = \gamma_j - \alpha_t^* - \pi$, and α_t^* is the angle of P_t with respect to the center of the neighboring cell. From (1), we can write

$$\theta'_t = \theta_t + \phi_t - \alpha_t, \quad (5)$$

$$\theta_t^* = \theta_t + \phi_t - \alpha_t^*. \quad (6)$$

4.2. Probability of handoff

Given the number of waypoints $X(\Delta t)$ that a node may reach during Δt , the probability of HO can be written as

$$\Pr\{\text{HO in } \Delta t\} = \sum_{i=0}^{\infty} \Pr\{\text{HO in } \Delta t | X(\Delta t) = i\} \cdot \Pr\{X(\Delta t) = i\}. \quad (7)$$

According to initial assumptions, $\Pr\{X(\Delta t) = i\}$ is zero for $i > 1$. Thus, Equation (7) can be written as

$$\begin{aligned} \Pr\{\text{HO in } \Delta t\} &= \Pr\{\text{HO in } \Delta t | X(\Delta t) = 1\} \cdot \Pr\{X(\Delta t) = 1\} \\ &\quad + \Pr\{\text{HO in } \Delta t | X(\Delta t) = 0\} \cdot \Pr\{X(\Delta t) = 0\} \\ &= \Pr\{\text{HO}a\} \cdot \Pr\{X(\Delta t) = 1\} \\ &\quad + \Pr\{\text{HO}b\} \cdot (1 - \Pr\{X(\Delta t) = 1\}), \end{aligned} \quad (8)$$

where $\Pr\{X(\Delta t) = 1\}$ represents the probability of reaching the waypoint during Δt , $\Pr\{\text{HO}a\}$ is the probability of HO given that a waypoint is reached during Δt , while $\Pr\{\text{HO}b\}$ is the probability of HO given that node moves on same direction and at same speed during Δt . Because the current direction of movement γ_j and the current speed v_j are known, $\Pr\{\text{HO}b\}$ only depends on the distance to the cell border in direction γ_j and can easily be calculated.

The flow charts in Figures 3 and 4 show the algorithm used to estimate the probability of HO, the probability of no HO, and the expressions used in each case. Depending on the node's direction of movement, the distance of P_t to A (x_A) is longer or shorter than the distance of P_t to the cell boundaries (x_t) (i.e., the node is moving towards the

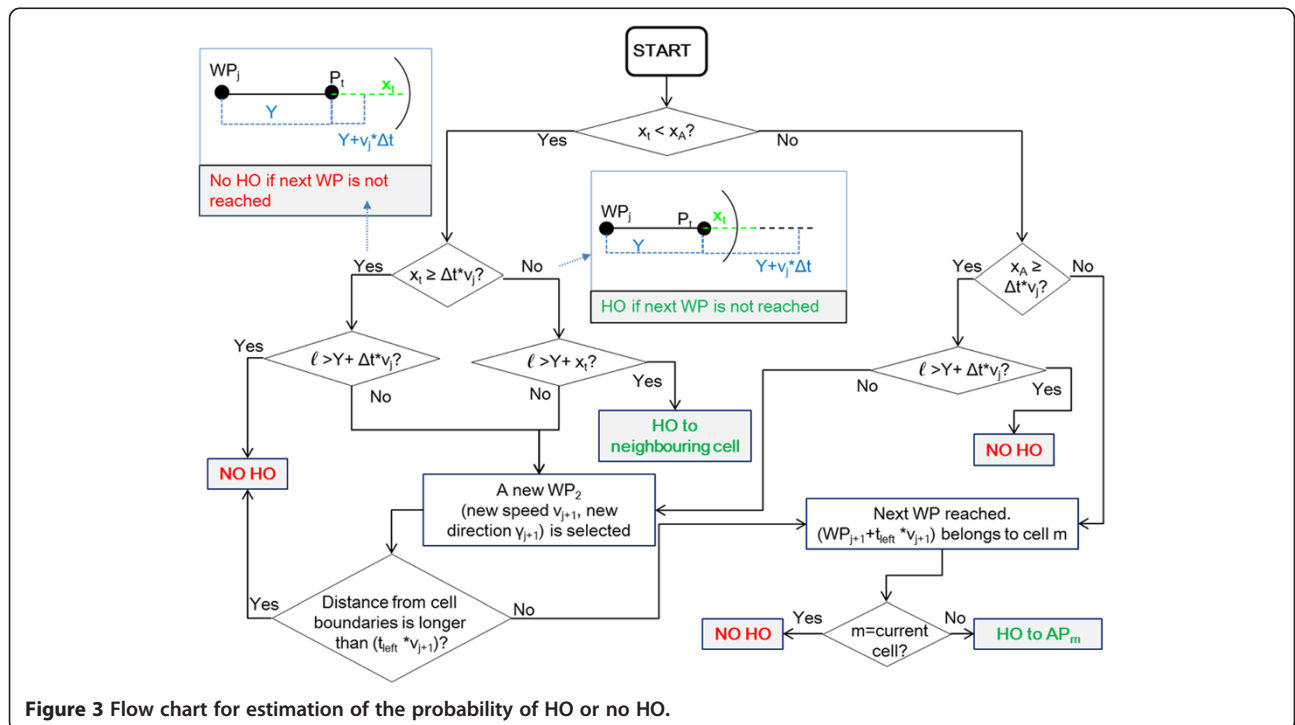
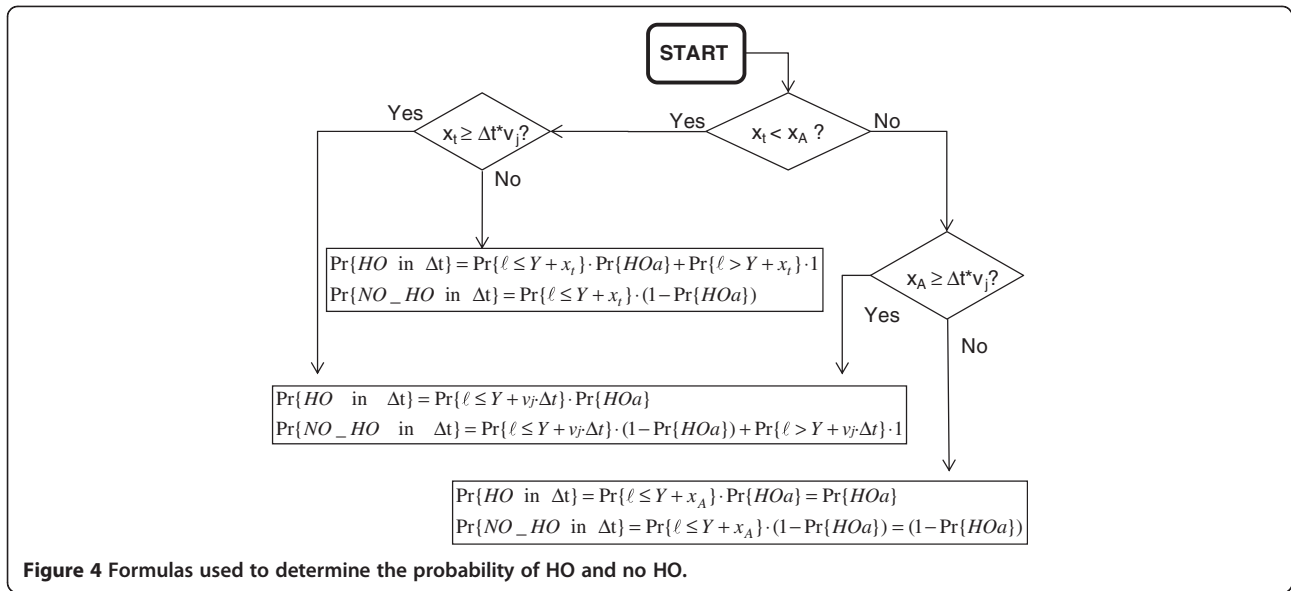


Figure 3 Flow chart for estimation of the probability of HO or no HO.



center of A or in opposite direction, respectively). Figure 3 shows that, in the first case ($x_t < x_A$), an HO is performed if the distance to the cell boundaries is shorter than the distance walked at given speed during Δt ($x_t < v_j \cdot \Delta t$) and the distance between two waypoints (ℓ) is longer than $Y + x_t$ (i.e., the node does not reach the waypoint before exiting its current cell, thus $\Pr\{HO_b\}$ is one). On the other hand, if $x_t \geq x_A$, then an HO is performed only if the distance to the boundaries of A is shorter than the distance walked at given speed during Δt ($x_A < v_j \cdot \Delta t$) and the point reached in the new direction falls outside the current cell. In all the other cases, the node will remain inside its current cell. In Figure 4, the corresponding expressions for each case are provided.

In the following sections, expressions for the probability of reaching the next waypoint and for $\Pr\{HO_a\}$ are provided.

4.2.1. Probability of reaching the next waypoint during Δt

Recall that the node is located at P_t at time t and that it has been traveling a distance Y from previous waypoint WP_j . The next waypoint may be located at any point on the straight line between P_t and $P_t + v_j \cdot \Delta t$ (if $x_t \geq v_j \cdot \Delta t$ and $x_t < x_A$), between P_t and $P_t + x_t$ (if $x_t < v_j \cdot \Delta t$ and $x_t < x_A$), or between P_t and $P_t + x_A$ (if $x_t \geq x_A$). We define this generic point on the current direction of movement at generic distance r from P_t as $S(r)$ (i.e., $S(r=0) \equiv P_t$). The expression $\Pr\{X(t+r/v_j) = 1\}$ represents the probability of reaching the next waypoint after traveling a distance r at current speed v_j , where $t + \frac{r}{v_j} \leq \Delta t$. This probability can be rewritten as the probability that the distance between two waypoints (ℓ) is shorter than a generic distance $L = Y + r$. Thus, depending on the geometry and on the current speed, we find different expressions

$$\Pr\{\text{reach the next waypoint during } \Delta t\} = \begin{cases} \Pr\{\ell \leq Y + x_t\} = \int_Y^{Y+x_t(\theta'_t)} f_L(l|\theta_t) dl & \text{if } x_t(\theta'_t) < v_j \cdot \Delta t \text{ and } x_t(\theta'_t) < x_A(\theta_t) \\ \Pr\{\ell \leq Y + x_A\} = \int_Y^{Y+x_A(\theta_t)} f_L(l|\theta_t) dl & \text{if } x_A(\theta_t) < v_j \cdot \Delta t \text{ and } x_t(\theta'_t) \geq x_A(\theta_t), \\ \Pr\{\ell \leq Y + v_j \cdot \Delta t\} = \int_Y^{Y+v_j \cdot \Delta t} f_L(l|\theta_t) dl & \text{if } x_t(\theta'_t) \geq v_j \cdot \Delta t \text{ or } x_A(\theta_t) \geq v_j \cdot \Delta t \end{cases} \quad (9)$$

where $f_L(\ell|\theta_t)$ is the pdf of the distance between two waypoints provided that the current direction of movement is known. According to [22], if A is a circle of radius R , $f_L(\ell|\theta_t) = \frac{8}{\pi^*R} \cdot \frac{1}{2 \cdot R} \left(\arccos\left(\frac{\ell}{2 \cdot R}\right) - \frac{\ell}{2 \cdot R} \cdot \sqrt{1 - \left(\frac{\ell}{2 \cdot R}\right)^2} \right)$.

4.2.2. Probability of HO when the waypoint is reached (Pr{HOa})

Consider that the node reaches the next waypoint at the generic point $S(r)$ at time $\left(t + \frac{r}{v_j}\right)$. We can define t_r as the remaining time before Δt elapses. It can take values between $(0, \Delta t)$. We can write

$$t_r = \Delta t - \frac{r}{v_j}. \tag{10}$$

The probability that the node reaches another waypoint during t_r is small when Δt is small. According to our initial assumption, by accurately choosing Δt , we can discard the possibility that another waypoint is reached, which would highly complicate the solution. The polar coordinates of the waypoint are (d_{WP}, Φ_{WP}) . At this point, a new waypoint will randomly be selected inside A and the node will start moving in a new direction. According to Bettstetter et al. [22], nodes take a non-uniformly distributed angle of direction at each new

waypoint. The pdf of this angle depends on the shape of A and the starting waypoint of the node. Thus, in a circular area of radius R , the pdf of the angle of direction γ is

$$f_\gamma(\gamma|(d_{WP}, \phi_{WP})) = f_\theta(\theta|d_{WP}) = \frac{1}{2\pi R^2} x_A^2(\theta_t). \tag{11}$$

Moreover, a new speed will randomly be selected at the waypoint. The points reached after t_r at maximum and minimum speed are estimated in each possible direction of movement. These points identify a crown where the node may be located after Δt . Since the speed is uniformly distributed between v_{min} and v_{max} , each point among $(v_{min} \cdot t_r)$ and $(v_{max} \cdot t_r)$ is equally probable. Each direction may be selected according to (11). The area where the node may move can be divided into two areas: one inside the current cell (i.e., no HO is performed) and another one inside one (at least) of the neighboring cells (i.e., an HO is performed). According to previous definitions, the latter is $\text{Pr}\{\text{HOa}|r\}$. As $S(r)$ moves away from P_t , the radius of the crown will decrease and the distances and angles will change. Thus, we have to evaluate $\text{Pr}\{\text{HOa}|r\}$ at any distance r from P_t . The final expression to estimate the probability of HO given that the waypoint is reached during Δt is

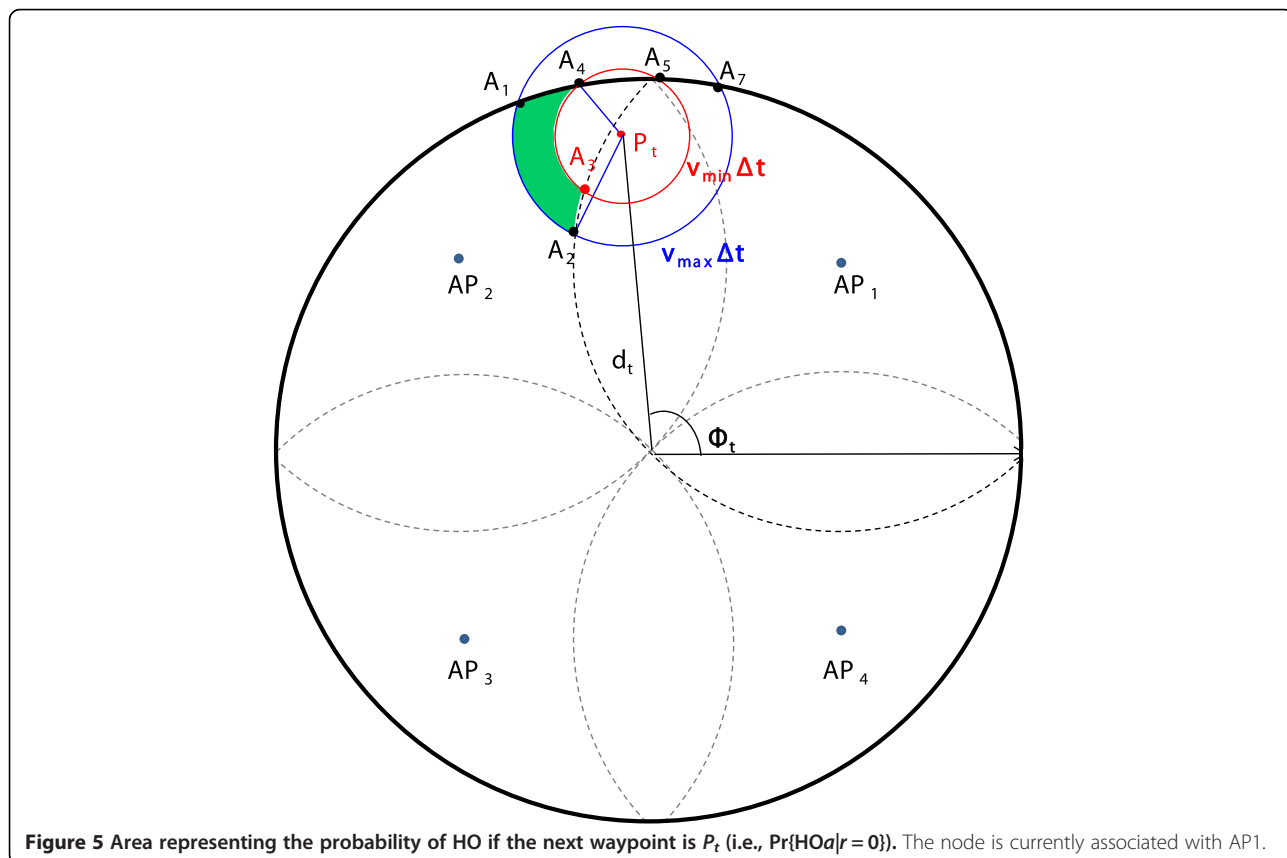


Figure 5 Area representing the probability of HO if the next waypoint is P_t (i.e., $\text{Pr}\{\text{HOa}|r=0\}$). The node is currently associated with AP1.

$$\Pr\{HOa\} = \begin{cases} \int_0^{v_j \cdot \Delta t} \Pr\{HOa|r\} \cdot f_R(r) dr & \text{if } x_t(\theta'_t) \geq v_j \cdot \Delta t \text{ and } x_t(\theta'_t) < x_A(\theta_t) \\ \int_0^{x_t(\theta'_t)} \Pr\{HOa|r\} \cdot f_R(r) dr & \text{if } x_t(\theta'_t) < v_j \cdot \Delta t \text{ and } x_t(\theta'_t) < x_A(\theta_t) \\ \int_0^{x_A(\theta_t)} \Pr\{HOa|r\} \cdot f_R(r) dr & \text{if } x_t(\theta'_t) \geq x_A(\theta_t), \end{cases} \quad (12)$$

where $\Pr\{HOa|r\}$ represents the probability of HO given that the next waypoint is $S(r)$, and $f_R(r)$ is the pdf of the possible positions $S(r)$. Note that the waypoints are uniformly selected in A .

4.3. Application to four APs

In order to illustrate how the analytical framework provides the forecast of the HO in a specific scenario, we will consider a layout with four APs. The coverage area of each AP is a circular area of radius $rcell$. The APs are located at the vertices of a square whose side is R , as shown in Figure 1. In Figure 5, the method to

calculate the probability of HO when the next waypoint is P_t (i.e., $\Pr\{HOa|r=0\}$) is illustrated. From the current point P_t , a circular crown can be drawn with inner radius $(v_{\min} \cdot \Delta t)$ and outer radius $(v_{\max} \cdot \Delta t)$. The crown represents the area where the node may be located if it changes its direction of movement and speed at P_t . Because the speed distribution is uniform between v_{\min} and v_{\max} , the distribution of the node locations' inside this area is uniform too. Points inside the crown but outside A are discarded (i.e., they fall outside the area of movement). Angles for the points $A1$, $A4$, $A5$, and $A7$ should be estimated; we refer to these angles as θ_{A1} , θ_{A4} ,

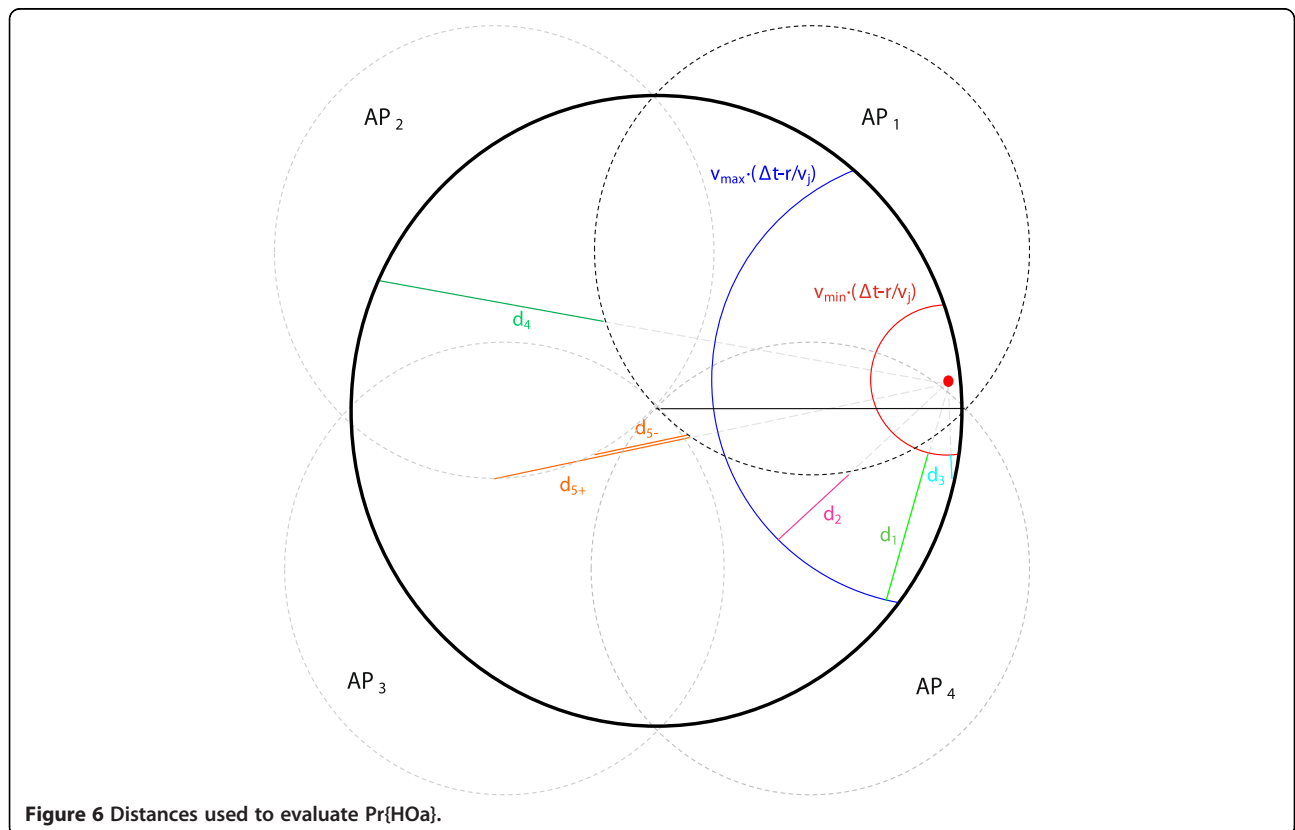


Figure 6 Distances used to evaluate $\Pr\{HOa\}$.

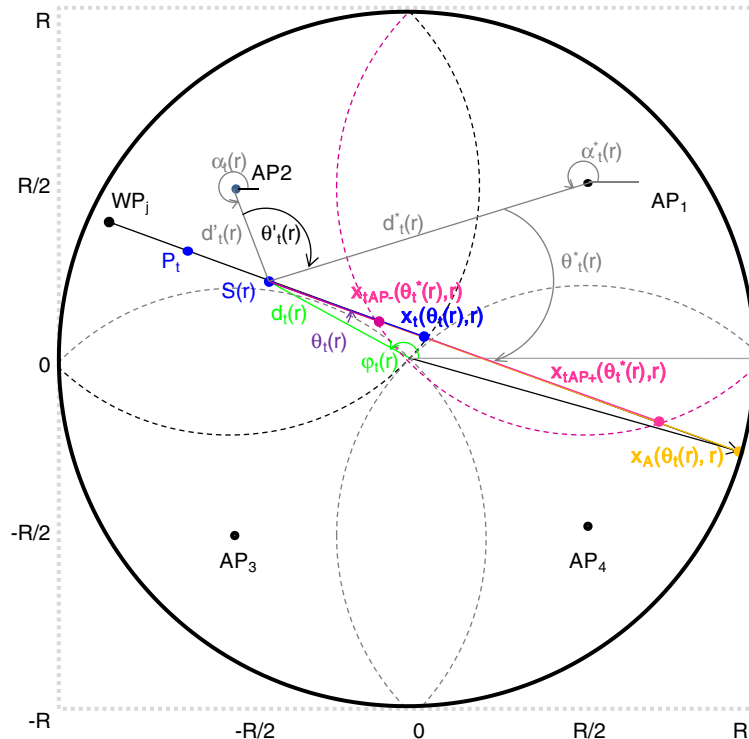


Figure 7 Distances from the cell boundary (x_t), whole area (x_A), and neighboring cell (x_{tAP}) in current direction γ_j at point $S(r)$.

θ_{A5} , and θ_{A7} , respectively. The HO area is represented in green in Figure 5 (i.e., the node is currently associated with AP1). It spans from angle θ_{A4} and θ_{A2} . The probability of HO in this case equals the probability of HO to AP2 and can be evaluated as

$$\Pr\{\text{HO}_A|r=0\} = \int_{\theta_{A4}}^{\theta_{A2}} f_{\Theta}(\theta|d_t(r)) \cdot \frac{\min(d1(r), d2(\theta, r), d3(\theta, r))}{\min(d1(r), d3(\theta, r))} d\theta \quad (13)$$

where r is the distance already walked from P_t (i.e., zero in this case), $d1(r)$ is the difference of the two radii of the crown (see Figure 6), $d2(\theta, r)$ is the difference between the outer radius of the crown and $x_t(\theta, r)$, $d3(\theta, r)$ is the difference of $x_A(\theta, r)$ and the inner radius of the crown, and θ represents all possible angles of movement from the current position with respect to the centre of A . $f_{\Theta}(\theta|d_t(r))$ is defined in (11) and represents the pdf of the direction angle θ provided that we are at distance $d_t(r)$ from the centre of A .

The integral in (13) cannot be evaluated because the integrand function changes in the interval of integration. Instead, a sum of integrals is used where the minimum function is substituted by the corresponding minimum distance at each interval (see Section 5). Expressions for

$d1(r)$, $d2(\theta, r)$, and $d3(\theta, r)$ are provided in Appendix 1. Depending on the current position of the node, the circular crown intersects the cell boundaries and/or A at different points. All of the other possible distances ($d4(\theta, r)$, $d5(\theta, r)$, $d6(\theta, r)$) are provided in Appendix 1. Refer to Figure 6 to better understand these values.

Equation 13) is evaluated iteratively at any point $S(r)$ according to (12). In each iteration, the time decreases as the node moves at speed v_j in direction γ_j ; then, the radius of the crown will decrease, and the distances and

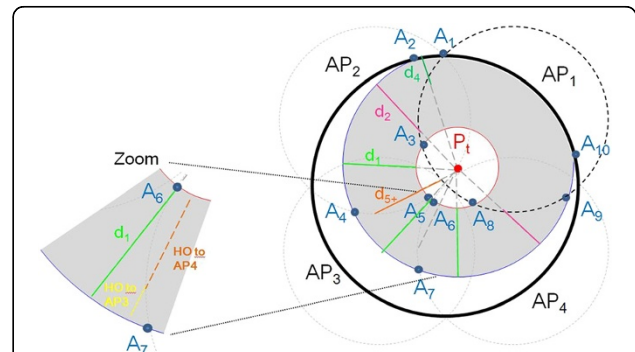


Figure 8 Example of calculation of $\Pr\{\text{HO}_A\}$ with an approximation in the estimation of $\Pr\{\text{HO}_{AP3}\}$ and $\Pr\{\text{HO}_{AP4}\}$ (i.e., $0.5 \cdot d_1$ is used instead of the exact distances displayed in yellow and orange in the zoom).

Table 1 Probability ϵ with which $X(\Delta t)$ is smaller or equal to one

Δt (s)	50	80	90	100
ϵ (%)	99.20	95.82	93.81	91.30

angles will change. Equations (2)–(4) for the generic case (i.e., the next waypoint is $S(r)$) are provided in Appendix 2. Figure 7 represents the distances previously defined according to $S(r)$.

5. Numerical examples

The analysis is implemented with Maple. The integrals in (12) are solved through numerical integration. As mentioned, the integral in (13) is split into a sum of integrals where the minimum function is substituted by the corresponding minimum distance. For that purpose, all possible cases are considered, and all possible combinations of angles are analyzed. As an example, Equation (13) is evaluated as

$$\begin{aligned} \Pr\{\text{HO}a|r=0\} &= \int_{\theta_{A4}}^{\theta_{A1}} f_{\theta}(\theta|d_t(0)) \cdot \frac{d3(\theta,0)}{d3(\theta,0)} d\theta \\ &+ \int_{\theta_{A3}}^{\theta_{A2}} f_{\theta}(\theta|d_t(0)) \cdot \frac{d2(\theta,0)}{d1(0)} d\theta \\ &+ \int_{\theta_{A1}}^{\theta_{A3}} f_{\theta}(\theta|d_t(0)) \cdot \frac{d1(0)}{d1(0)} d\theta \end{aligned} \quad (14)$$

In a few cases, due to the complexity of the geometry, an approximation is applied in the estimation of the probability of HO. Figure 8 shows an example in which

the approximation is used (i.e., for the probability of HO to AP3 and AP4). These probabilities are computed as

$$\begin{aligned} \Pr\{\text{HOAP3}a|r=0\} &= \int_{\theta_{A4}}^{\theta_{A5}} f_{\theta}(\theta|d_t(0)) \cdot \frac{d2(\theta,0) - d5^+(\theta,0)}{d1(0)} d\theta \\ &+ \int_{\theta_{A5}}^{\theta_{A6}} f_{\theta}(\theta|d_t(0)) \cdot \frac{d1(0)}{d1(0)} d\theta \\ &+ 0.5 \cdot \int_{\theta_{A6}}^{\theta_{A7}} f_{\theta}(\theta|d_t(0)) \cdot \frac{d1(0)}{d1(0)} d\theta, \end{aligned} \quad (15)$$

$$\begin{aligned} \Pr\{\text{HOAP4}a|r=0\} &= \int_{\theta_{A7}}^{\theta_{A8}} f_{\theta}(\theta|d_t(0)) \cdot \frac{d1(0)}{d1(0)} d\theta \\ &+ \int_{\theta_{A8}}^{\theta_{A9}} f_{\theta}(\theta|d_t(0)) \cdot \frac{d2(\theta,0)}{d1(0)} d\theta \\ &+ 0.5 \cdot \int_{\theta_{A6}}^{\theta_{A7}} f_{\theta}(\theta|d_t(0)) \cdot \frac{d1(0)}{d1(0)} d\theta, \end{aligned} \quad (16)$$

where in both equations the last term stands for the approximation (see zoom in Figure 8).

The time Δt is selected such that, with a given probability ϵ , it is guaranteed that the node will reach no more than one waypoint during Δt . Since the pdf of the time between two waypoints is known [22,25], Δt is found by solving

$$\Pr\{\Delta t \leq T1 + T2\} \leq \epsilon, \quad (17)$$

Table 2 Values and numerical results for the five cases analyzed with Maple

Cases	1	2	3	4	5
P_t	(1; $3\pi/4$)	(2; $7\pi/4$)	(138; 0)	(1; $3\pi/2$)	(138; $\pi/4$)
WP_j	(63; $7\pi/4$)	(140; $7\pi/4$)	(138; π)	(10; $3\pi/2$)	($70\sqrt{2}$; $\pi/4$)
Δt (s)	10	10	60	80	10
v_j (m/s)	1.4	1	2	2	1
γ_j	135°	135°	0°	90°	45°
x_t (m)	197	2	2	1	60
x_A (m)	139	142	2	141	2
Y (m)	64	138	276	9	39
Current cell	2	4	1	4	1
$Pr\{\text{HOAP1}\}$ (%)	0.83	0.62	[70.06]	99.90	[100]
$Pr\{\text{HOAP2}\}$ (%)	[98.28]	97.43	0	0.02	0
$Pr\{\text{HOAP3}\}$ (%)	0.83	0.62	0	0.04	0
$Pr\{\text{HOAP4}\}$ (%)	0.06	[1.32]	29.94	[0.04]	0

Values in square brackets stand for the probability of remaining in current cell.

Table 3 Average percentages of HO and no HO for the five cases simulated with Matlab

Cases	1	2	3	4	5
$Pr\{HOAP1\}$ (%)	0.64	0.46	[73.80]	99.65	[100]
$Pr\{HOAP2\}$ (%)	[98.76]	98.08	0.00	0.08	0.00
$Pr\{HOAP3\}$ (%)	0.58	0.49	0.00	0.11	0.00
$Pr\{HOAP4\}$ (%)	0.02	[0.98]	26.20	[0.16]	0.00

Values in square brackets stand for the probability of remaining in current cell.

where T_1 and T_2 represent the timestamp (clock) of the first and of the second transitions, respectively. Table 1 shows the values for different probabilities of no more than one HO. In the cases presented below, this probability is set to a minimum of 95%.

For the numerical cases, R is set to 140 m. The mobility pattern is RWP with a uniform speed distribution between 0.7 and 2 m/s and a pause time of zero. The area is served by four APs as shown in Figure 1 (e.g., AP1 placed at point (70; 70) with respect to the centre of A). The cell range is $70\sqrt{2}$ m. After the equations in [22,25], the mean distance between two waypoints is equal to 126.756 m, the average time-weighted speed is 1.238 m/s and the mean time between two waypoints is equal to 102.292 s.

In order to present numerical results that illustrate some interesting cases, we selected five representative cases. The selected cases are far from representing all possible scenarios but are enough to support and facilitate a better understanding of the theoretical results. Table 2 shows the initial conditions for the cases under study. Polar coordinates are provided for P_t and WP_j . Both x_t and x_A are provided to show which calculation is performed (refer to Figure 4). The probability of HO to any cell is provided. Because the probability of HO to the current cell is obviously zero, the value provided in Table 2 corresponds to the probability of remaining (i.e.,

no HO) and is enclosed in square brackets to avoid misunderstandings. The same notation is also used in Tables 3 and 4. The results are discussed after providing a better understanding of each case through Figure 9.

The five cases are depicted in Figure 9. The blue and red circles represent the maximum and minimum distances the node can walk if moving in any direction during Δt at maximum and minimum speeds, respectively. The grey area represents all the possible points that the node can reach during Δt . The blue arrow represents the current direction of the movement. The current association to a cell is marked with darker boundaries. In cases 1 and 2, the node can take any direction and any speed without exiting A , while in the other cases there are directions and speeds that bring the node outside A (i.e., it changes direction and speed before exiting A). The green star represents $P_t + v_j \cdot \Delta t$ (i.e., no waypoint is reached during Δt)

In case 1, the node has just entered cell 2 and it will HO only if it reaches a waypoint. As shown in Figure 9, if the node changes direction in P_t , it has roughly a 60% of chances to HO. While moving in the same direction, the probability of HO given that node changes direction will decrease (i.e., the grey crown shown in Figure 9 gets smaller as time elapses and its center moves toward the green star); this explains the low values for the probabilities of HO. Moreover, due to the symmetry of the layout, the probabilities of HO to AP1 and AP3 are the same, while the probability of HO to AP4 is very low.

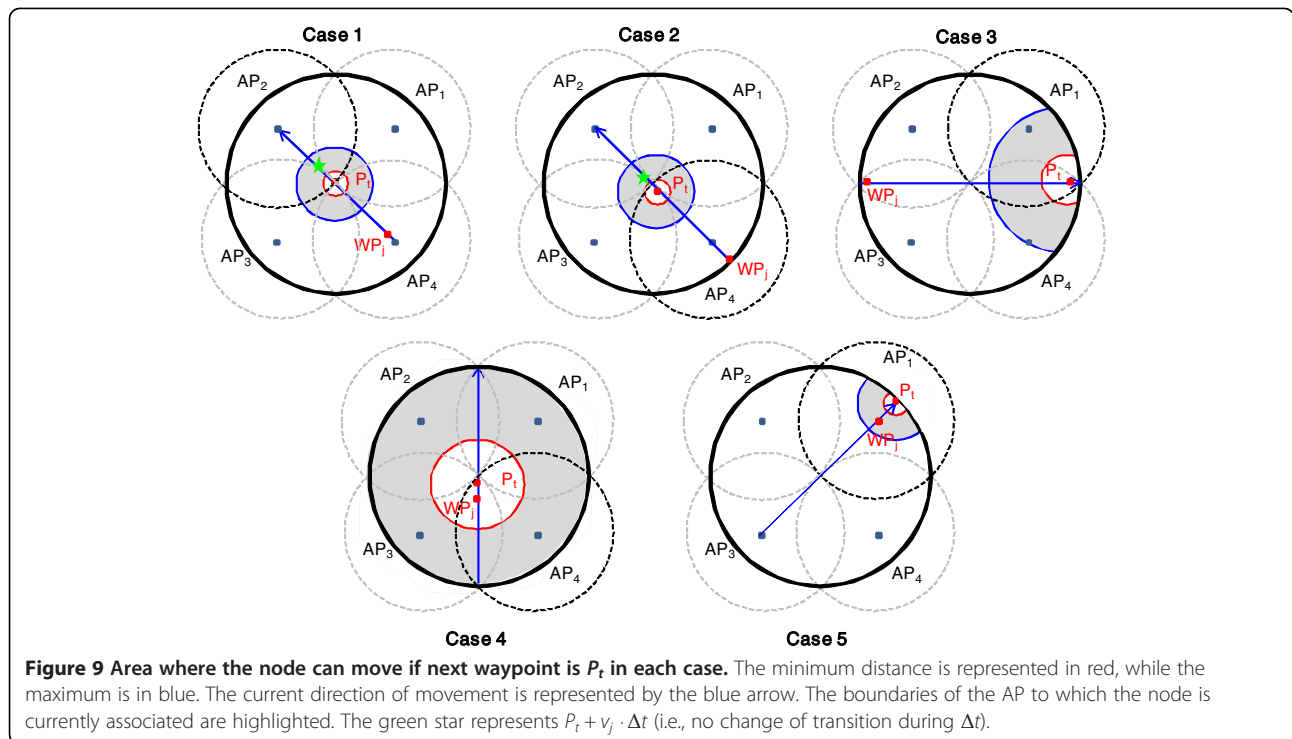
In case 2, the node is approaching the border of cell 4 toward cell 2, so HO is highly probable. Only if the node reaches the waypoint before exiting cell 4, it has some chances of remaining in the current cell or HO to AP1 or AP3. This explains the very low probabilities of HO.

In case 3, the node is reaching the boundaries of A , so the probability of reaching the waypoint during Δt is

Table 4 Values for the other five cases analyzed with Maple and Matlab

Cases	6	7	8	9	10
P_t	(105; 0.74π)	(85; 0.26π)	(30; $\pi/2$)	(80; $3\pi/2$)	(30; $\pi/4$)
WP_j	(130; 0.72π)	(130; 0.22π)	(80; $\pi/4$)	(80; $5\pi/4$)	(20; $7\pi/4$)
Δt (s)	60	80	80	50	80
v_j (m/s)	1.3	1.3	0.9	1.2	1.8
γ_j	295°	303°	205°	337°	79°
x_t (m)	105.71	84.82	18.42	28.93	148.71
x_A (m)	235.80	216.55	150.09	88.29	114.05
Y (m)	26.06	46.90	53.20	61.23	36.06
Current cell	2	1	1	3	1
$Pr\{HOAP1\}$ (%)	0.75 0.35	[20.77] [22.02]	[3.78] [2.73]	0.02 0.01	[63.85] [57.00]
$Pr\{HOAP2\}$ (%)	[98.46] [99.21]	68.20 70.76	90.43 93.66	0.14 0.06	19.59 25.30
$Pr\{HOAP3\}$ (%)	0.78 0.44	2.04 0.96	2.48 1.20	[18.66] [15.06]	5.35 3.21
$Pr\{HOAP4\}$ (%)	0.01 0.00	8.99 6.27	3.31 2.40	81.18 84.87	11.21 14.50

Values in square brackets stand for the probability of remaining in current cell.



close to one. Since it is associated to cell 1 and the HO starts when the node leaves the cell, the percentage of HO to AP4 (29.94%) is lower than the percentage of no HO—recall that it is shown inside square brackets in Table 2. Even at maximum speed, the node has no time to reach cell 2 or cell 3, so the probability of HO to them is zero.

Case 4 is similar to case 2. The percentage of HO is very high (99.96%) since the node is approaching the border of its cell. Since the boundaries of cells 4 and 2 overlap at only one point (i.e., the center of A), the node will HO to AP1 with much higher probability. On the other hand, the probabilities of HO to AP2 and AP3 only accounts for the few chances that the node has to reach the waypoint before exiting its current cell.

Finally, case 5 is similar to case 3. Again, the node will reach the waypoint because it is moving toward the boundaries of A . Because Δt is short, the node has no opportunity to leave its cell, so the probability of HO is zero. This case differs from the others in that the node is not walking through the center of A .

6. Simulation results

The five cases analyzed are simulated with Matlab in order to evaluate the loss of accuracy produced by the necessary simplifications to the analytical model: numerical integration in (13), the approximation when the geometry is too complex, etc. Each simulation run consists of 5,000 samples and 10 independent repetitions

for each run are performed for each case. This simulation length is long enough to guarantee a confidence interval better than 95% with a margin smaller than 10% in all cases. Table 3 shows the average percentages of HO—note that the value in square brackets represents the probability of remaining in the current cell.

All of the results from simulation match the analytical results. Due to the approximation in the analysis, slight differences may be noticed among the simulation and analytical results. Still, the error in the estimation of the probability of HO in the analysis with respect to that in the simulation is always lower than 4% (case 3). Thus, the simulation validates the analytical model.

For a more comprehensive validation, other five cases (see Figure 10) are analyzed both analytically and through simulation, and the results are presented in Table 4. The error in the probability of HO or no HO is always less than 7% (case 10). These results confirm that the proposed analytical framework is valid and that the approximations and simplifications followed have only a slight impact on the results.

7. Conclusion

An analytical model for the estimation of the probability of HO to a given cell of a node moving according to the RWP mobility model has been investigated. The method is presented for a layout in which the overall area is a circle with four APs located at the corners of a square inside it. It is assumed that the position and timestamp

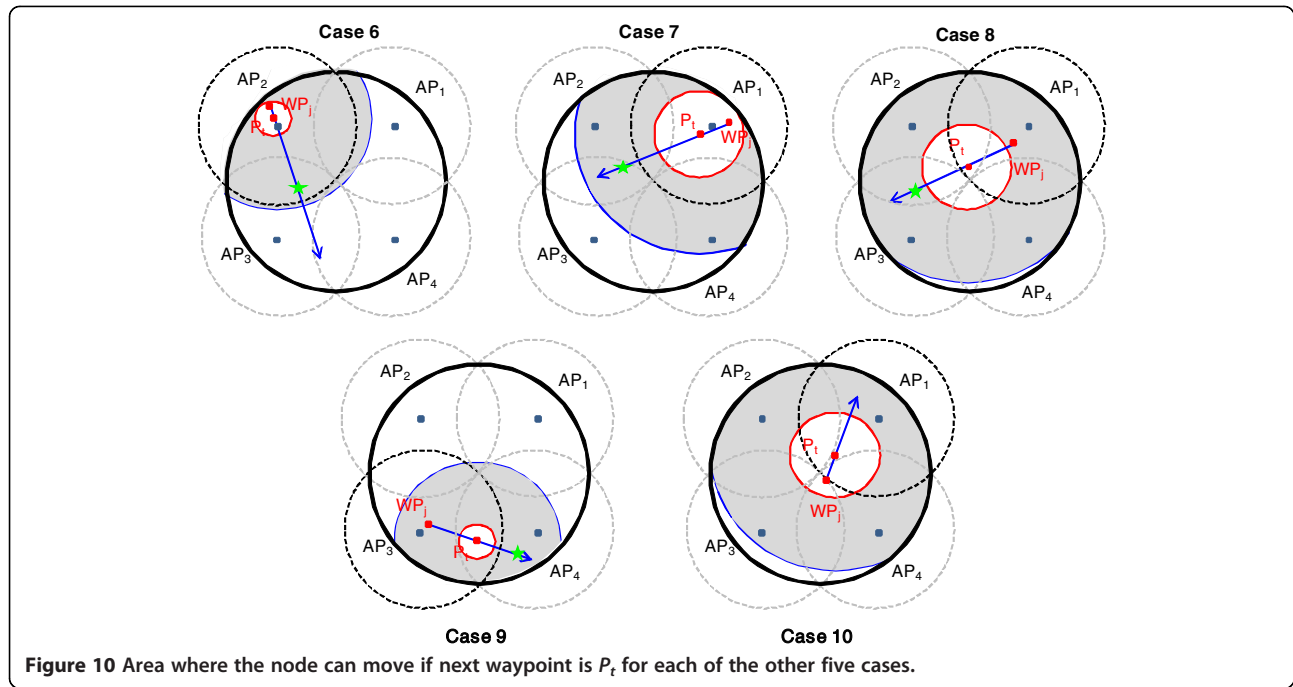


Figure 10 Area where the node can move if next waypoint is P_t for each of the other five cases.

of the last waypoint are known. The model can be generalized to any symmetrical layout with overlapping areas, where the APs are placed at the corners of a regular polygon (i.e., triangle, hexagon). In this article, equations are provided for the case in which the speed distribution is uniform, the pause time is zero, and propagation conditions are ideal (i.e. only path loss). Numerical results for several cases have been presented and compared with simulations to validate the approximations assumed in the mathematical analysis. This study provides the research community with an analytical framework which can improve the understanding and use of the RWP mobility model used in the majority of simulation studies with moving nodes. From a practical perspective, it can be used to improve resource allocation in cellular networks, thus smoothing the HO procedure and improving the QoS.

Appendix 1

Expressions for the distances used in the evaluation of the probability of HO in (13) are

$$d1(r) = \frac{1}{2} \left(\Delta t - \frac{r}{v_j} \right)^2 \cdot (v_{\max}^2 - v_{\min}^2), \quad (18)$$

$$d2(\theta, r) = \frac{1}{2} \left(\left(v_{\max} \cdot \left(\Delta t - \frac{r}{v_j} \right) \right)^2 - x_t^2(\theta'_t, r) \right), \quad (19)$$

$$d3(\theta, r) = \frac{1}{2} \left(x_A^2(\theta, r) - \left(v_{\min} \cdot \left(\Delta t - \frac{r}{v_j} \right) \right)^2 \right). \quad (20)$$

According to the geometry, other distances may be used for the evaluation of $\Pr\{HOa\}$

$$d4(\theta, r) = \frac{1}{2} \left(x_A^2(\theta, r) - x_t^2(\theta'_t, r) \right), \quad (21)$$

$$d5(\theta, r) = \frac{1}{2} \left(x_{tAP}^2(\theta_t^*, r) - x_t^2(\theta'_t, r) \right), \quad (22)$$

$$d6(\theta, r) = \frac{1}{2} \left(\left(v_{\max} \cdot \left(\Delta t - \frac{r}{v_j} \right) \right)^2 - x_{tAP}^2(\theta_t^*, r) \right). \quad (23)$$

Refer to Figure 6 for better understanding of these values.

Appendix 2

Generalization of Equations (2) to (4) in case the change of direction of movement and speed starts at $S(r)$ leads to the following equations

$$x_A(\theta_t(r), r) = d_t(r) \cdot \cos(\theta_t(r)) + \sqrt{R^2 - (d_t(r) \cdot \sin(\theta_t(r)))^2}, \quad (24)$$

$$x_t(\theta'_t(r), r) = d'_t(r) \cdot \cos(\theta'_t(r)) + \sqrt{r_{\text{cell}}^2 - (d'_t(r) \cdot \sin(\theta'_t(r)))^2}, \quad (25)$$

$$x_{tAP\pm}(\theta_t^*(r), r) = d_t^*(r, AP) \cdot \cos(\theta_t^*(r)) \pm \sqrt{r_{\text{cell}}^2 - (d_t^*(r, AP) \cdot \sin(\theta_t^*(r)))^2}, \quad (26)$$

where $d_t(r)$ is the distance of $S(r)$ to the center of A , $\theta_t(r)$ is the new direction of movement, $d'_t(r)$ is the distance of $S(r)$ to the center of the current cell, and $d_t^*(r, AP)$ is the distance of $S(r)$ to the border of the neighboring cell AP (as two intersections may occur, the symbol \pm stands for the two solutions). $\theta'_t(r)$ and $\theta_t^*(r)$ are derived from (5) and (6), respectively. Refer to Figure 7 for a better understanding of these values.

Competing interests

The authors declare that they have no competing interests.

Acknowledgments

This research was supported by the Spanish Government and ERDF through CICYT projects TEC2009-08198. The authors would like to thank Dr. Javier Ozón Gorrioz for his suggestions and valuable help with the mathematical analysis. Part of this study has been presented at IEEE LCN conference in October, 2011 [23].

Received: 5 June 2012 Accepted: 7 January 2013

Published: 25 January 2013

References

1. A Sgora, D Vergados, Handoff prioritization and decision schemes in wireless cellular networks: a survey. *IEEE Commun. Surv. Tutor.* **11**(4), 57–77 (2009)
2. A Mishra, M Shin, W Arbaugh, An empirical analysis of the IEEE 802.11 MAC layer handoff process. *SIGCOMM Comput. Commun. Rev.* **33**(2), 93–102 (2003)
3. H Velayos, G Karlsson, Techniques to reduce the IEEE 802.11b handoff time, in *Proceedings of the IEEE International Conference on Communications*, vol.7, 2004, pp. 3844–3848
4. Y Iraqi, R Baoutaba, Handoff and call dropping probabilities in wireless cellular networks, in *Proceedings of the IEEE International Conference on Wireless Networks, Communications and Mobile Computing*, vol.1, 2005, pp. 209–213
5. WS Soh, HS Kim, QoS provisioning in cellular networks based on mobility prediction techniques. *IEEE Commun. Mag.* **41**(1), 86–92 (2003)
6. DB Johnson, DA Maltz, Dynamic source routing in ad hoc wireless networks. Kluwer Academic Publishers *Mob. Comput.* **353**, 153–181 (1996)
7. S Kurkowski, T Camp, M Colagrosso, MANET simulation studies: the incredibles. *SIGMOBILE Mob. Comput. Commun. Rev.* **9**(4), 50–61 (2005)
8. T Ali, M Saquib, C Sengupta, Vertical handover analysis for voice over WLAN/cellular network, in *Proceedings of the IEEE International Conference on Communications*, ed. by, 2010, pp. 1–5
9. C Tong, JW Niu, GZ Qu, X Long, XP Gao, Complex networks properties analysis for mobile ad hoc networks. *IET Commun.* **6**(4), 370–380 (2012)
10. Q Min, R Zimmermann, An adaptive strategy for mobile ad hoc media streaming. *IEEE Trans. Multimed.* **12**(4), 317–329 (2010)
11. A Jindal, K Psounis, Contention-aware performance analysis of mobility-assisted routing. *IEEE Trans. Mob. Comput.* **8**(2), 145–161 (2009)
12. DN Alparslan, K Sohraby, Two-dimensional modeling and analysis of generalized random mobility models for wireless ad hoc networks. *IEEE/ACM Trans. Netw.* **15**(3), 616–629 (2007)
13. K Tae-Hyong, Y Qiping, L Jae-Hyoung, P Soon-Gi, S Yeon-Seung, A mobility management technique with simple handover prediction for 3 G LTE systems, in *Proceedings of the IEEE 66th Vehicular Technology Conference*, ed. by, 2007, pp. 259–263
14. A Rojas, P Branch, G Armitage, Validation of the random waypoint mobility model through a real world mobility trace, in *Proceedings of the IEEE Region 10 TENCN*, ed. by, 2005, pp. 1–6
15. T Camp, J Boleng, V Davies, A survey of mobility models for ad hoc network research. *Wirel. Commun. Mob. Comput. (WCMC) (Special Issue on Mobile Ad Hoc Networking)* **2**(5), 483–502 (2002)
16. F Bai, N Sadagopan, A Helmy, IMPORTANT: a framework to systematically analyze the impact of mobility on performance of routing protocols for adhoc networks, in *Proceedings of the Twenty-Second Annual Joint Conference of the IEEE Computer and Communications* **2**, 825–835 (2003)
17. TK Madsen, FHP Fitzek, R Prasad, Impact of different mobility models on connectivity probability of a wireless ad hoc network, in *Proceedings of the International Workshop on Wireless Ad-Hoc Networks*, ed. by, 2004, pp. 120–124
18. P Lassila, E Hyttiä, H Koskinen, Connectivity properties of random waypoint mobility model for ad hoc networks, in *Proceedings of the Fourth Annual Mediterranean Workshop on Ad Hoc Networks*, ed. by, 2005, pp. 159–168
19. V Pla, V Casares-Giner, Analytical-numerical study of the handoff area sojourn time. in *Proceedings of the IEEE Global Telecommunications Conference* **1**, 886–890 (2002)
20. E Hyttiä, J Virtamo, Random waypoint mobility model in cellular networks. *ACM/Kluwer Wirel. Netw.* **13**(2), 177–188 (2007)
21. E Zola, F Barcelo-Arroyo, Impact of mobility models on the cell residence time in WLAN networks, in *Proceedings of the IEEE Sarnoff Symposium*, ed. by, 2009, pp. 1–5
22. C Bettstetter, H Hartenstein, X Pérez-Costa, Stochastic properties of the random waypoint mobility model. *ACM/Kluwer Wirel. Netw. (Special Issue on Modeling and Analysis of Mobile Networks)* **10**(5), 555–567 (2004)
23. E Zola, F Barcelo-Arroyo, Probability of handoff for users moving with the random waypoint mobility model, in *Proceedings of the IEEE LCN*, 2011, pp. 187–190
24. C Bettstetter, G Resta, P Santi, The node distribution of the random waypoint mobility model for wireless ad hoc networks. *IEEE Trans. Mob. Comput.* **2**(3), 257–269 (2003)
25. E Hyttiä, P Lassila, J Virtamo, Spatial node distribution of the random waypoint mobility model with applications. *IEEE Trans. Mob. Comput.* **5**(6), 680–694 (2006)
26. W Yueh-Ting, H Tsung-Yen, L Wanjiun, T Cheng-Lin, Epoch, length of the random waypoint model in mobile ad hoc networks. *IEEE Commun. Lett.* **9**(11), 1003–1005 (2005)
27. S Sangho, AG Forte, R Anshuman Singh, H Schulzrinne, Reducing MAC layer handoff latency, in *IEEE 802.11 wireless LANs*, in *Proceedings of the ACM Second International Workshop on Mobility Management & Wireless Access Protocols*, 2004, pp. 19–26
28. K Ramachandran, S Rangarajan, JC Lin, Make-before-break MAC layer handoff in 802.11 wireless networks, in *Proceedings of the IEEE ICC*, vol.10, 2006, pp. 4818–4823
29. L Yong, G Lixin, Practical schemes for smooth MAC layer handoff in 802.11 wireless networks, in *Proceedings of the IEEE Computer Society International Symposium on World of Wireless, Mobile and Multimedia Networks*, 2006, pp. 181–190
30. J Márquez-Barja, C Calafate, JC Cano, P Manzoni, An overview of vertical handover techniques: algorithms, protocols and tools. *Elsevier. Comput. Commun.* **34**(8), 985–997 (2011)
31. X Yan, YA Şekercioğlu, S Narayanan, A survey of vertical handover decision algorithms in Fourth Generation heterogeneous wireless networks. *Elsevier Comput. Netw.* **54**(11), 1848–1863 (2010)
32. S Lee, K Kim, K Hong, D Griffith, YH Kim, N Gollmie, A probabilistic call admission control algorithm for WLAN in heterogeneous wireless environment. *IEEE Trans. Wirel. Commun.* **8**(4), 1672–1676 (2009)
33. R Ben Ali, S Pierre, On the impact of soft vertical handoff on optimal voice admission control in PCF-based WLANs loosely coupled to 3 G networks. *IEEE Trans. Wirel. Commun.* **8**(3), 1356–1365 (2009)
34. PN Pathirana, AV Savkin, S Jha, Mobility modelling and trajectory prediction for cellular networks with mobile base stations, in *Proceedings of the 4th ACM International Symposium on Mobile Ad Hoc Networking & Computing*, 2003, pp. 213–221
35. T Joshi, A Mukherjee, DP Agrawal, Exploiting mobility patterns to reduce re-authentication overheads in infrastructure WLAN networks, in *Proceedings of the IEEE Canadian Conference on Electrical and Computer Engineering*, 2006, pp. 1423–1426

36. S Michaelis, C Wietfeld, Comparison of user mobility pattern prediction algorithms to increase handover trigger accuracy, in *Proceedings of the IEEE Vehicular Technology Conference*, vol.2, 2006, pp. 952–956
37. MS Sricharan, V Vaidehi, A pragmatic analysis of user mobility patterns in macrocellular wireless networks. Elsevier *Pervas. Mob. Comput.* **4**(5), 616–632 (2008)
38. PS Prasad, P Agrawal, Movement prediction in wireless networks using mobility traces, in *Proceedings of the 7th IEEE Conference on Consumer Communications and Networking Conference*, 2010, pp. 1–5
39. S Libo, D Kotz, J Ravi, H Xiaoning, Evaluating next-cell predictors with extensive wi-fi mobility data. *IEEE Trans. Mob. Comput.* **5**(12), 1633–1649 (2006)
40. W Navidi, T Camp, Stationary distributions for the random waypoint mobility model. *IEEE Trans. Mob. Comput.* **3**(1), 99–108 (2004)

doi:10.1186/1687-1499-2013-16

Cite this article as: Zola et al.: Forecasting the next handoff for users moving with the Random Waypoint mobility model. *EURASIP Journal on Wireless Communications and Networking* 2013 **2013**:16.

Submit your manuscript to a SpringerOpen[®] journal and benefit from:

- ▶ Convenient online submission
- ▶ Rigorous peer review
- ▶ Immediate publication on acceptance
- ▶ Open access: articles freely available online
- ▶ High visibility within the field
- ▶ Retaining the copyright to your article

Submit your next manuscript at ▶ springeropen.com
